Laboratory-Scale Pipe Rheometry: A Study of a Microfibrillated Cellulose Suspension

Sanna Haavisto*, Johanna Liukkonen*, Ari Jäsberg*, Antti Koponen*, Martina Lille** and Juha Salmela*

Technical Research Centre of Finland, P.O. Box 1603, 40101 Jyväskylä, Finland

Addresses: * P.O. Box 1603, 40101 Jyväskylä, Finland. ** P.O. Box 1000, 02044 VTT, Finland

Email: forename.surname@vtt.fi

In this study a novel laboratory-scale pipe rheometer is utilized in rheological characterization of concentrated MFC and cellulose suspensions. The method is based on a combination of pulsed ultrasound velocity profiling (UVP) and pressure difference measurement (PD). The rheological properties of the suspensions are described in terms of pressure loss, viscosity and yield stress. The results are compared to rotational rheometer results. It is demonstrated that a well controlled pipe flow environment together with the UVP-PD technique is efficient in characterizing the rheological flow behavior of complex slurries.

Keywords: inline rheology, ultrasonic velocity profiling, microfibrillated cellulose

1 INTRODUCTION

Ultrasound velocity profiling (UVP) has been accepted as an important measuring technique in fluid dynamics and engineering applications. Furthermore, UVP is increasingly being used together with pressure difference measurement as a non-invasive rheological measuring technique commonly known as UVP-PD. This non-invasive method is capable of in-line rheological measurements for concentrated, opaque fluids in real-time [1-5].

Cellulose fibers generally form an opaque flocculated suspension with high viscosity already at low mass concentrations. In many cases conventional rheometers fail to produce reliable information for these suspensions. Recently, both UVP and UVP-PD methods have been successfully applied in probing details of cellulose fiber suspension flows and their rheological properties [6-9].

Recent developments in cellulose fiber disintegration have facilitated the production of micro- and nanofibrillated cellulose (MFC/NFC). The properties of these fibrils differ significantly from cellulose fibers, especially in specific surface area, aspect ratio, strength and flexibility [10]. Development of new materials, processes and applications utilizing MFC/NFC requires deeper understanding of the rheological properties of these suspensions.

The aim of this study was to develop a laboratory-scale rheometer with minimal limitations in terms of sample properties (sample quantity, consistency range, viscosity and particle dimensions) and which enables repeatable measurements in varying shear conditions. A tube flow geometry was selected due to its practical significance in process industry and its effortless modification and scalability. The UVP-PD method was preferred due to its applicability to opaque fluids. Furthermore, UVP-PD is based on direct measurements and requires no assumptions concerning the flow profile or boundary conditions.

While the qualitative rheological behavior of virgin wood fiber suspensions is well known, the rheology of strongly fibrillated fiber suspensions (micro / nano-suspensions) is still mostly unknown. The novel pipe rheometer is applied in this study to the analysis of the rheological properties of commercial MFC at consistencies from 0.2% to 1.5%. The rheological properties of the suspensions are described in terms of pressure loss behavior, yield stress and viscosity. The results are compared with rotational rheometer results for MFC and with pipe rheometer results for a birch cellulose suspension.

2 MATERIALS

The microfibrillated cellulose used in this study is the commercial product Celish® KY-100G (Daicel Chemical Industries, Japan) made from purified wood pulp (see Figure 1b). The average length and width of Celish® fibers are 350 µm and 15 µm respectively [11]. The fiber surfaces are, however, very strongly fibrillated (see Figure 1c). The size distribution of these fibrils is very wide ranging from microscale to nanoscale.

As a reference for MFC, bleached birch cellulose (see Figure 1a) was measured in similar conditions to 1.5% MFC pulp. The approximate average fiber length and width are 0.9 mm and 20 µm, respectively. The fiber surfaces have fibrils, but are very smooth when compared to MFC. Coarseness of birch fibers is 114 mg/mm).

Before measurement, the cellulose fibers were dispersed in deionized water and disintegrated. The temperature of the slurries was 20±0.5 °C.

The mobility of fibers in a suspension can often be estimated using the crowding factor

$$N_{cr} = \frac{2}{3} c_v \left(\frac{L}{d} \right)^2 \approx \frac{5 c_m L^2}{\varpi} \ , \tag{1}$$

where *L* is fiber length, *d* is fiber diameter, ω is fiber coarseness, and $c_{v,m}$ is the volume/mass concentration of the suspension [15]. There are a number of well-documented crowding factor regions. In a suspension with a crowding factor below one, individual fibers undergo minimal interaction and flow properties are not affected by other fibers. *Martinez et al.* [16,17] defined the 'gel crowding factor' $N_{cr} = 16$ where fiber suspension behavior changes from dilute behavior to behavior where fibers interact significantly with each other. Still, at this range fibers do not become immobilized. This occurs at sedimentation consistency $N_{cr} \approx 60$.

The crowding factor of birch pulp at 1.5% mass consistency is 53. The birch suspension is, i.e., close to its sedimentation consistency. As the crowding number has been derived for smooth rod-like fibers, it is a too simplistic parameter for multi-scale material like MFC suspension which is gel-like already at 0.3% consistency (at this consistency N_{cr} for MFC is only 1.6 using the same coarseness as for birch fibers).

3 METHODS

3.1 Theory of pipe rheometry

The experimental results acquired from a pipe rheometer can be analyzed using different approaches, including the use of rheological models as described, for example, by Wiklund et al. [4]. In this study, the results are presented based on direct measurements. The results are analysed in two ways. Firstly, in the traditional way only the pressure loss and volumetric flow rate data are used assuming a laminar parabolic velocity profile. For a laminar Newtonian flow in a straight tube, the ***apparent shear rate*** $\dot{\gamma}_a$ and shear stress τ_W at the tube wall are given by

$$\dot{\gamma}_a = \frac{4Q}{\pi R^3} \tag{2}$$

$$\tau_W = \frac{\Delta P R}{2L} \tag{3}$$

where Q is the volumetric flow rate, R is the radius of the tube and ΔP is the pressure difference over the length L of the tube. The ***shear viscosity*** is the ratio of shear stress to shear rate,

$$\mu_a = \tau_W / \dot{\gamma}_a \ . \tag{4}$$

This analysis corresponds to conventional viscosity measurements using, for example, a capillary viscometer. In this analysis no corrections due to non-Newtonian profile or slip are applied. The result is referred to as the ***apparent viscosity***.

The second analysis utilizes the experimental mean velocity profile and thereby gives the viscosity measured locally in the flow. This method includes no assumptions concerning the flow profile or boundary conditions. The local shear rate $\dot{\gamma}(r)$ is obtained directly from the velocity profile. As the shear stress at each distance from the tube wall is

$$\tau(r) = \tau_W (1 - r/R), \tag{5}$$

the shear viscosity can be calculated locally. This result is referred as the ***intrinsic viscosity***

$$\mu(r) = \tau(r) / \dot{\gamma}(r) \ . \tag{6}$$

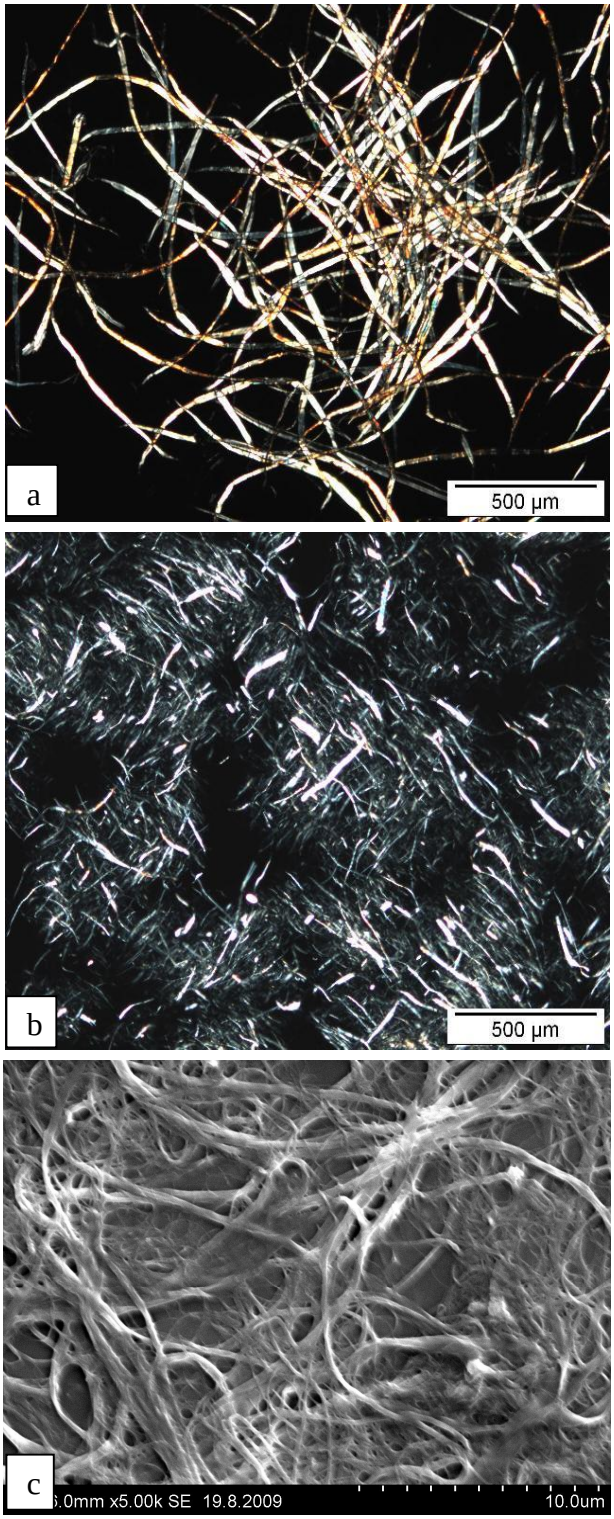

***Figure 1**. A polarized light microscope image of birch cellulose (a), MFC (b) and a SEM image of MFC (c).*

3.2 Novel laboratory-scale pipe rheometer

A schematic diagram of the novel laboratory-scale pipe rheometer is shown in Figure 2. The pipe rheometer consists of two chambers connected by a replaceable vertical pipe section. The volume of each chamber is

approximately 3 liters. The measurement pipe used in this study was a smooth acrylic tube with an inner diameter of 16 mm.

The measurement is initiated by filling the bottom chamber with the sample fluid. The fluid is then pumped to the upper chamber. Here, the desired filling level is determined by an ultrasound surface detector. The measurement is started by opening the valve downstream of the measurement tube. The flow in the measurement tube can be driven by gravity or by overpressure in the upper chamber. The flow rate of the gravity driven flow is controlled by an air valve and the pressure driven flow is controlled via a pressure regulator. This ensures that the flow in the measurement tube is undisturbed by, for example, pump pressure surges.

The mass flow rate of the fluid is determined by three weight sensors and the volume flow rate by an ultrasound surface detector. The pressure difference in the measurement tube is measured over a distance of 0.90 m.

Rheological characterization of the fluid is carried out using the UVP-PD method. The region of steady flow is determined from the measurement data and analyzed for mean pressure loss, mass rate and volumetric flow rate. The result is combined with the simultaneously measured mean velocity profile.

The operation of the pipe rheometer, starting from sample loading to execution of the user-defined measurement scheme and sample removal, is fully automated. The measurement scheme can cover a range of processing conditions within a single measuring period.

3.3 Ultrasound velocity profiling

The velocity profiles are measured using a pulsed UVP system (DOP2000, Signal-Processing S.A., Switzerland). The settings used for the velocity measurements are summarized in Table 1. Depending on the flow speed, typically 100–1000 individual profiles are recorded and analyzed for each measurement.

***Table 1**: Main UVP settings*

Setting	Value
Sensor base frequency	8 MHz
Sensor active diameter	5 mm
Doppler angle	80°
Pulse Repetition Frequency (PRF)	1–2.7 kHz
Burst length	4 cycles

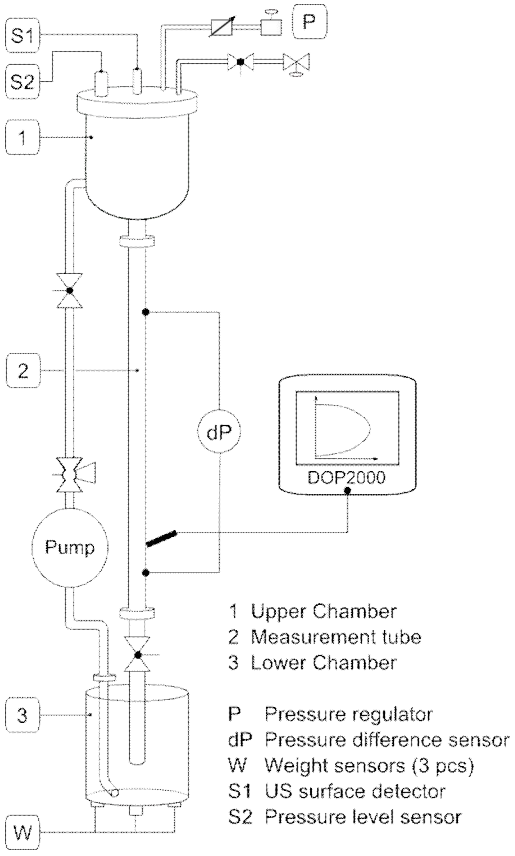

***Figure 2**. Schematic diagram of the laboratory-scale pipe rheometer.*

3.4 Verification measurements

The effect of entrance length was studied by measuring the fluid velocity profile at five locations between the measurement tube inlet and the lower pressure loss measurement point. Here, several MFC concentrations and flow rates were used. It was found, that in all cases the velocity profile was completely saturated between the pressure loss measurement points.

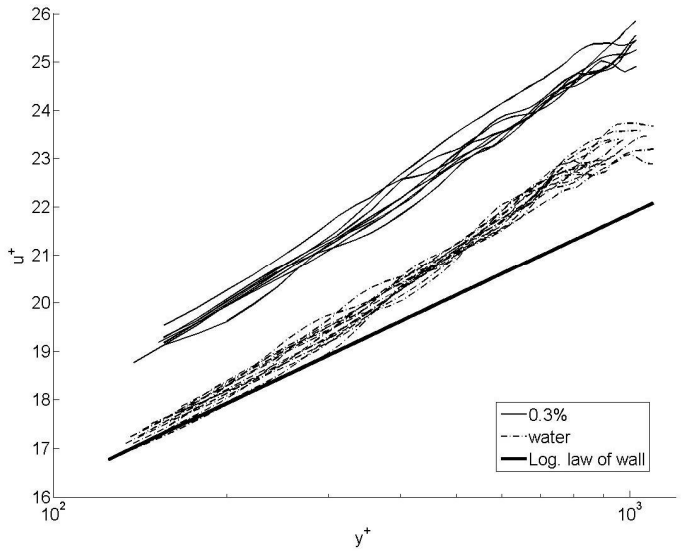

***Figure 3.** Velocity profiles (u^+ as a function of y^+) for pure water and 0.3% for MFC. The solid line shows the theoretical log law of wall curve for water. The flow rate varies between 2.0 m/s and 3.0 m/s.*

In Figure 3, (turbulent) velocity profiles of pure water and 0.3% MFC are shown. Here the following commonly used notation has been used:

$$y^+ = \frac{yu^*}{\nu}, \quad u^+ = \frac{u}{u^*}, \quad u^* = \left(\frac{\tau_w}{\rho}\right)^{1/2}, \tag{7}$$

Above *y* is the distance from the wall, υ is the kinematic viscosity of water, *u* is the fluid velocity, ρ is the fluid density, and τ_w is the wall shear stress. We see from Figure 3 that with small values of y^+ the measured velocity profile of water matches closely with the theoretical log law of wall curve of turbulent Newtonian flows. With high values of y^+ the measurements separate from the theoretical curve, as expected [12].The unphysical bumps appearing in the velocity profiles are supposedly caused by secondary reflections of the ultrasonic signal from the pipe wall. They can probably be eliminated by improving the acoustical contact between the ultrasonic sensor and the pipe wall.

3.5 Reference measurements with a conventional rheometer

The viscosity of the MFC dispersion was measured at 20 °C with a stress controlled rotational rheometer (AR-G2, TA Instruments) equipped with a vane geometry (Figure 4). The diameters of the cylindrical sample cup and vane were 30 mm and 28 mm, respectively. The length of the vane was 42 mm. (In Figure 4c another typical measurement geometry, plate geometry, is also show.)

After loading the sample into the measuring geometry it was allowed to rest for 5 min before the measurement was started. For the determination of yield stress (Figure 14), the steady state flow behavior was measured with a gradually increasing shear stress in the range 0.01-100 Pa. For 1.5% MFC an additional shear viscosity measurement was performed in strain controlled mode with a gradually increasing shear rate in the range 10^{-4} - 100 s^{-1} (Figure 6).

We see from Figures 7 and 14, that the viscosity and yield stress results for MFC obtained from UVP-PD and the rotational rheometer correlate closely with each other.

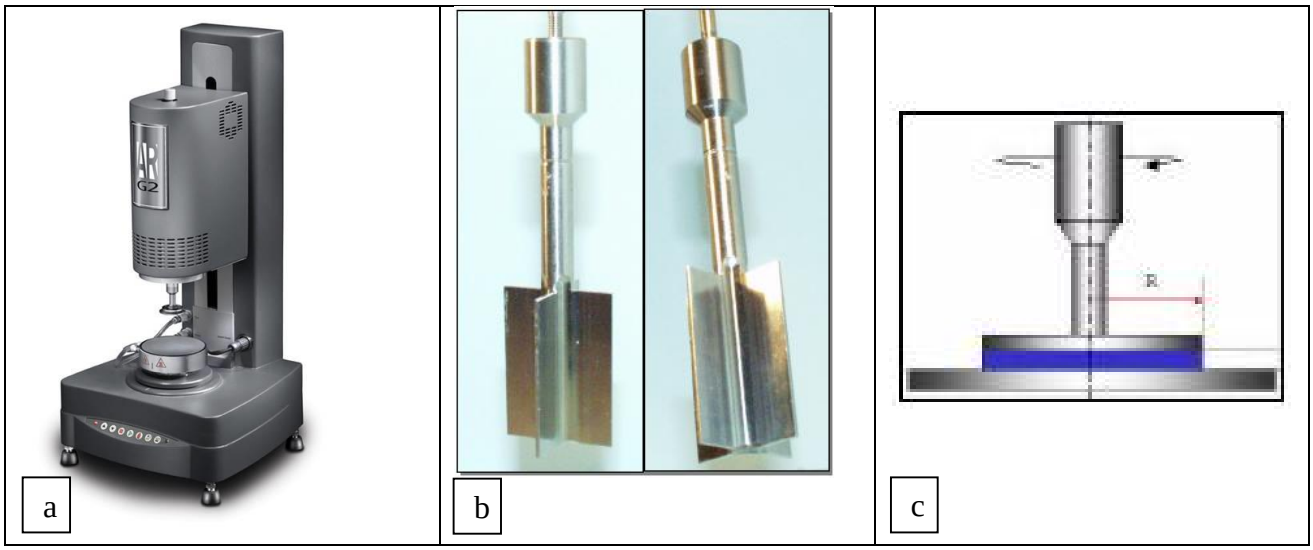

Figure 4*. a) AR-G2 TA Instruments rheometer. b) Vane geometry c) Plate geometry.*

4 PRESSURE LOSS BEHAVIOR OF TRADITIONAL WOOD FIBER SUSPENSIONS

Traditional wood fiber suspensions are pseudoplastic fluids, i.e. the behavior of their intrinsic viscosity is generally shear thinning. Concentrated wood fiber suspensions ($N_{cr} > 60$) are also Bingham fluids, as they exhibit yield-stress behavior.

The qualitative flow behavior of concentrated wood fiber suspensions in a straight tube is relatively well

known (see Figure 5). Quantitatively, however, the flow behavior is much more complicated than that of a pure Newtonian fluid [7]. If the pressure gradient applied to the tube is below a characteristic threshold value (this value being dependent on the fiber type and concentration) the fiber plug does not move. In this case, the motion of the carrier fluid is described as flow through porous medium (which often causes pipe plugging). Above a threshold pressure, the fiber plug is set in motion. The fibers are initially in direct contact with the wall, inducing high shear stress and thus high losses. As the flow rate is increased plug flow behavior is preserved, but a thin layer of pure water (a 'lubrication layer') is created next to the wall. Characteristic of this flow regime, the wall friction is approximately constant and may even decrease with increasing flow velocity. The flow velocity typically needed for this effect increases with increasing suspension consistency. As the flow rate increases further, turbulent flow appears near the walls and the surface of the fiber plug begins to break. Thus, in this mixed flow regime a turbulent fiber annulus surrounds a rigid fiber plug in the middle of the tube. At some point, frictional loss falls below that of the carrier liquid and a drag reduction regime is obtained. As the flow rate is further increased, the solid fiber core gradually vanishes, indicating a fully turbulent or 'fluidized' flow regime. Here, the loss typically approaches the pure fluid curve asymptotically as the flow rate is increased.

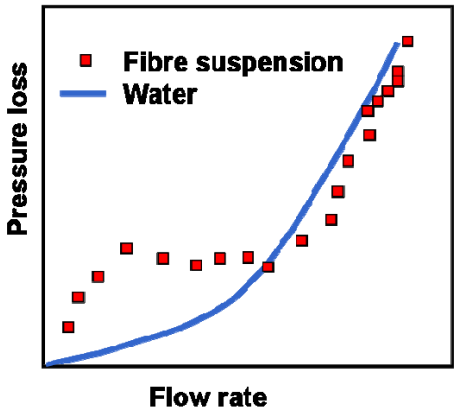

Figure 5*. Qualitative behavior of pressure loss as a function of flow rate for a fully developed flow of a concentrated wood fiber suspension in a straight smooth tube. The solid line indicates the standard pressure loss behavior of water.*

5 RESULTS

5.1 Comparison of MFC and birch cellulose at 1.5% consistency

The pressure drop of 1.5% MFC and birch cellulose is shown as a function of mean flow velocity in Figure 6. While there is a substantial difference in the pressure loss magnitudes of MFC and birch cellulose, the qualitative pressure loss behaviors are similar and follow the general picture explained in Section 4, where: at the lowest flow rates the pressure losses depend linearly on the flow rate (region I); then there exists a velocity region of approximately constant pressure loss (between regions II and III); and, finally, the pressure loss starts to increase again (regions IV and V). The only clear difference in pressure loss curves is the sudden pressure loss drop of MFC (at $v \approx 0.1\ \mathrm{m/s}$) which is not seen with birch cellulose here. Similar pressure loss drops, albeit not so strong, are often seen with long fiber suspensions, e.g. with pine pulps [7].

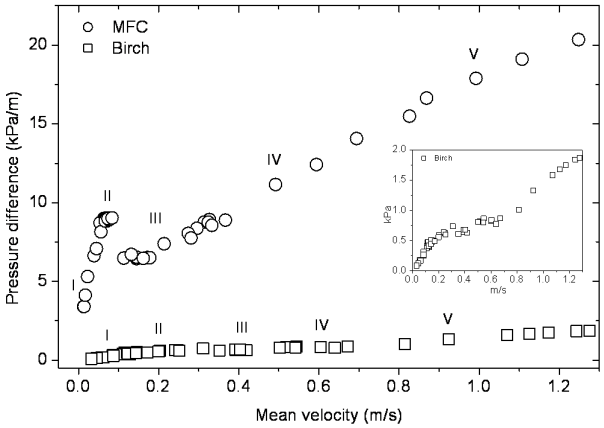

***Figure 6**. Pressure drop for a 1.5% suspension as a function of mean velocity. The roman numerals indicate different velocity regimes (birch magnified in the small window).*

The viscosity results for 1.5% MFC and birch pulp are presented in Figure 7. The highest apparent Reynolds numbers $\mathrm{Re}_a = \rho u D / \mu_a$ for 1.5% MFC and birch cellulose, determined from Eqs. (2)-(4), are 200 and 700, respectively. As expected from the pressure loss results, the viscosity of MFC is clearly higher than that of birch cellulose. For both suspensions, viscosity is strongly dependent on shear rate. In addition, the apparent viscosity agrees qualitatively with the other results.

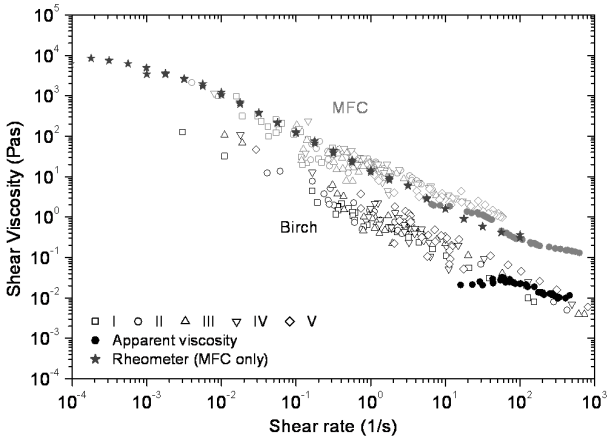

***Figure 7.** Intrinsic (open symbols) and apparent (solid symbols) shear viscosities for birch cellulose (black) and MFC (gray) at 1.5% consistency. The roman numerals refer to the different velocity regimes shown in Figure 6.*

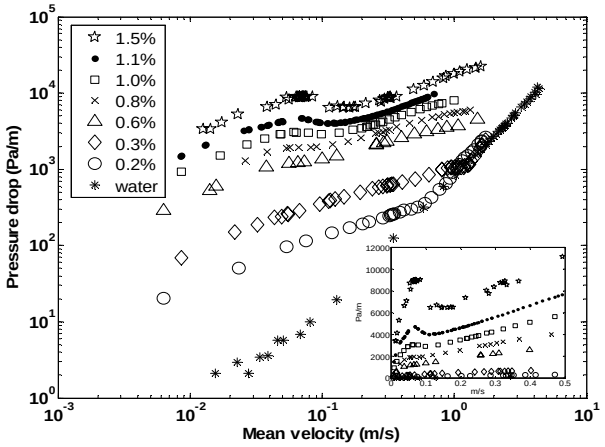

***Figure 8**. Pressure drop for MFC as a function of mean velocity*.

5.2 Rheology of MFC

In Figure 8, the pressure drop for MFC is shown as a function of mean velocity for several consistencies. The corresponding curve for water is also shown for comparison. It can be seen that the flow behavior of MFC deviates significantly from that of water at all consistencies. In general, the loss for MFC is strongly dependent on consistency. At low flow rates, the loss for MFC is considerably higher than that for water in all cases. For consistencies up to 0.8%, the loss increases monotonously with flow rate. For consistencies above 0.8%, there is a drop in the loss curve (at $v \approx 0.1\ \mathrm{m/s}$). For the lowest consistency 0.2% pressure loss approaches exactly that of water at high flow rates. For 0.3% the pressure loss drops even below that of water with the highest flow rates. This is also seen in Figure 4. The strength of this drag reduction effect (DR) is seen more clearly in Figure 9.

The qualitative behavior of MFC thus appears reasonably similar to a normal wood fiber suspension. One difference is that for MFC the pressure drop in the loss curve takes place with all consistencies with the same mean flow velocity.

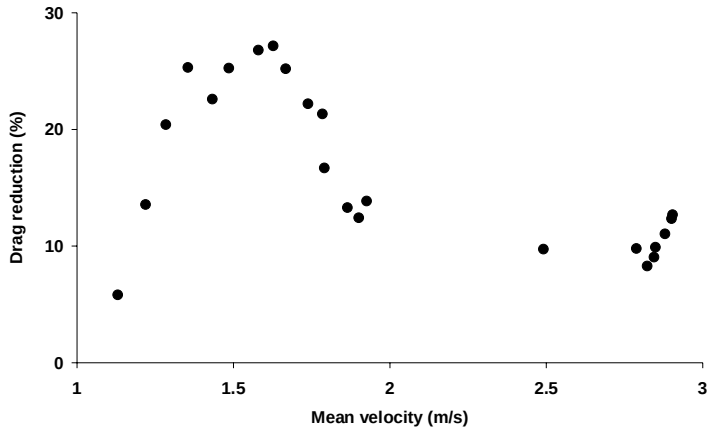

Figure 9. *DR-effect for 0.3% MFC.*

Figures 10 and 11 shows the development of velocity profiles with increasing flow rate for consistencies 0.3% and 1.0%. This behavior can be explained as follows. In both cases there is plug flow at the lowest flow velocities. Then, as the wall shear stress exceeds the yield stress of the suspension, the suspensions begin to break close to the walls and the profiles begin to round. As the flow rate increases further, the wall-fiber interactions [13,14] grow high enough (at $v \approx 0.1\ \mathrm{m/s}$) to push fibers away from the pipe walls. With the 1.0% suspension, this seems create a lubrication layer on the pipe surfaces. As a result, the pressure loss decreases. Simultaneously, the velocity profile returns to plug flow as the shear stress at the boundaries of the fiber suspension decrease. Probably due to higher fiber mobility, this does not seem to occur in the 0.3% suspension. Finally, with the highest flow rates, the pipe flow starts to become turbulent, initially close to the walls. As a result, the velocity profiles resemble that of turbulent water flow, and profiles become more blunt for 0.3% and more rounded for 1.0% suspensions, respectively. In this area MFC fibers absorb a fraction of the turbulent eddies, causing the DR-effect with 0.3% suspensions.

The dynamics of MFC suspension flows can be further understood by calculating their Metzner-Reed Reynolds number. This has been done in the Appendix.

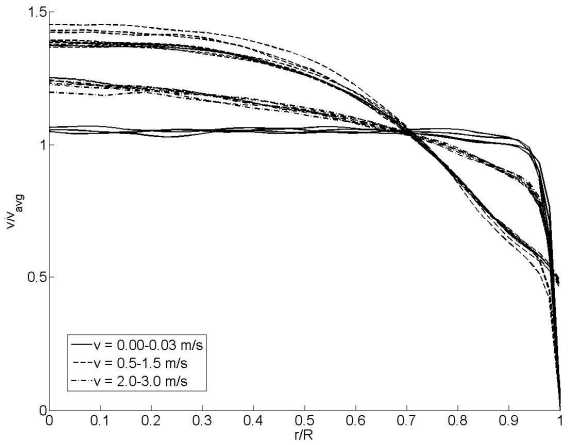

***Figure 10**. Velocity profiles for 0.3% MFC.*

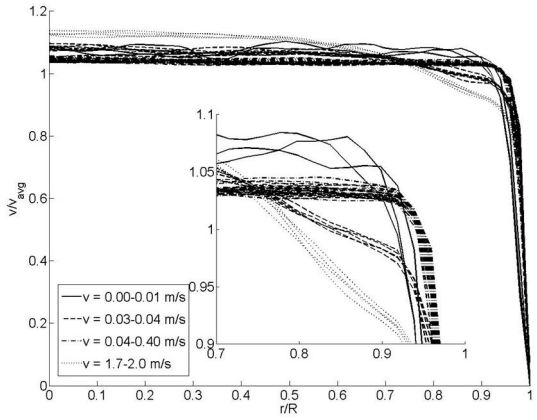

***Figure 11**. Velocity profiles for 1.0% MFC.*

The yield stress τ_y can be obtained from pipe flow measurements using the formula

$$\tau_y = \tau_W \left(1 - R_0/R\right), \tag{8}$$

where R_0 is the radial position at which the fiber plug brakes. R_0 can be estimated from the velocity profiles. Figure 12 shows R_0 as a function of flow rate for consistencies 0.3% and 1.1%. As expected, R_0 grows monotonously as a function of flow rate for lower consistency. For the higher consistency the behavior is more complicated due to the temporary drop in the pressure loss curve.

The yield stresses of MFC solutions, calculated from Eq. (8), are shown in Figure 13. We see here that yield stresses tend to increase with increasing flow rate at the lowest consistencies. The reason for this behavior is not known, but it might be due to memory effects related to low-consistency MFC suspensions. The experiments have been performed minute-wise from low velocity to high velocity sequentially. This means that the shearing history of MFC has been different in each measurement.

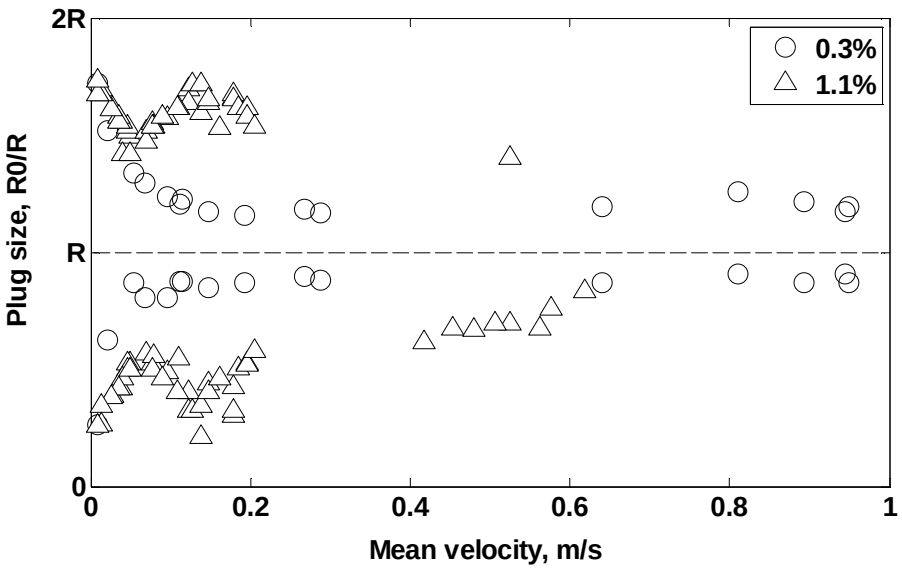

***Figure 12**. Location of the plug boundary (R_0) as a function of MFC suspension flow rate for consistencies 0.3% and 1.1%.*

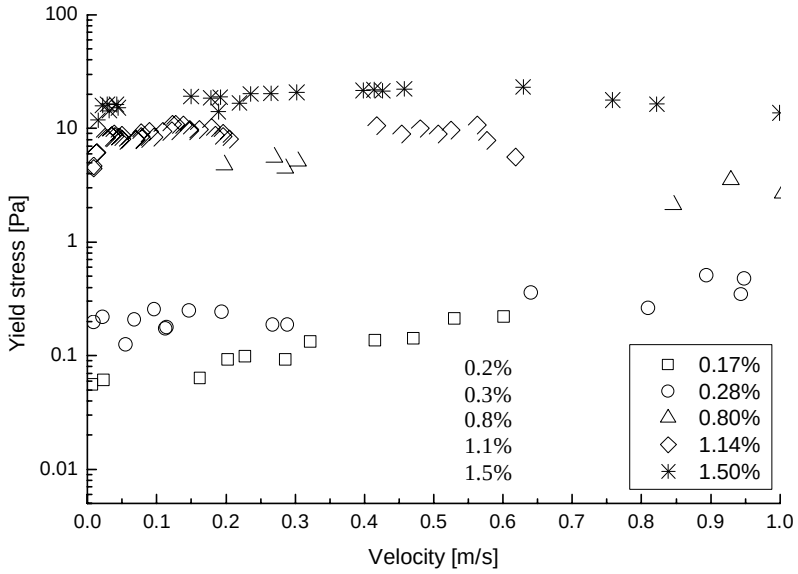

***Figure 13.** Yield stress as a function of flow rate for MFC suspensions.*

The (logarithmic) averages of MFC yield stress obtained with the pipe rheometer are compared in Figure 14 with the results of the vane geometry rheometer. Results from Ref. [11], obtained with a plate geometry rheometer, have also been shown for comparison. The results of the pipe and vane geometry are shown to correlate closely, whereas the results of the plate geometry have given significantly lower values. The most probable explanation for this discrepancy is differences between the analyzed MFC samples. Another possible cause is unsuitability of the used plate geometry for measuring the rheology of MFC due. Wall depletion may be another reason for the lower yield stress values obtained with the plate geometry.

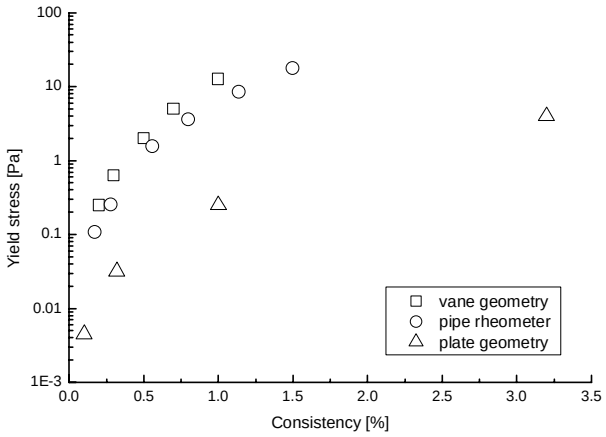

***Figure 14**. Yield stress as a function of consistency for MFC suspensions. The plate geometry results are taken from Ref. [11].*

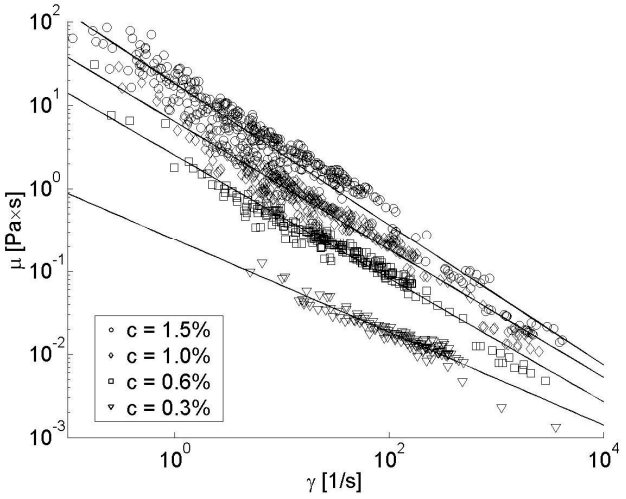

***Figure 15.** Intrinsic shear viscosities for different consistencies of MFC.*

Figure 15 shows the intrinsic shear viscosities for different consistencies of MFC. The pipe flow rates were between 0.25 m/s and 1.5 m/s. We can see from Figure 15 that MFC suspensions are strongly shear thinning at all consistencies and shear thinning behavior increases with concentration. We also see that the intrinsic viscosities increase strongly with increasing consistency. The dependence of viscosity on shear rate can be described with the power law

$$\mu = K\dot{\gamma}^{n-1}, \tag{9}$$

where *K* and *n* are the ***consistency index*** and ***flow index***, respectively [4]. Table 2 shows these parameters for different MFC consistencies. Notice that Eq. (9) is valid only for shear stresses that are clearly higher than yield stress. For 0.3% MFC, for example, this limit is reached at $\dot{\gamma} \approx 1\frac{1}{s}$.

***Table 2**. Consistency index K and flow component n for different MFC consistencies.*

Consistency %	0.3	0.6	1.0	1.5
K	0.24	2.5	6.4	18
n	0.44	0.26	0.23	0.15

6 CONCLUSIONS

This study used a novel laboratory-scale pipe rheometer for rheological characterization of concentrated MFC and cellulose suspensions. The method is based on a combination of pulsed ultrasound velocity profiling and pressure difference measurement. The rheological properties of the suspensions were described in terms of pressure loss, viscosity and yield stress. The results were compared to rotational rheometer results. It was demonstrated that a well controlled pipe flow environment together with the UVP-PD technique is an effective mean of characterizing the rheological flow behavior of complex slurries in process-like environments.

REFERENCES

[1] Ouriev B, Windhab EJ: Rheological study of concentrated suspensions in pressure-driven shear flow using a novel in-line ultrasound Doppler method, Experiments in Fluids 32 (2002) 204-211.

[2] Brunn P, Wunderlich T, Müller M: Ultrasonic rheological studies of a body lotion, Flow Measurement and Instrumentation 15 (2004) 139-144.

[3] Pfund D, Greenwood MS, Bamberger JA, Pappas RA: Inline ultrasonic Rheometry by pulsed Doppler, Ultrasonics 44 (2006) e477-e482.

[4] Wiklund J, Shahram I, Stading M: Methodology for in-line Rheology by ultrasound Doppler velocity profiling and pressure difference techniques, Chemical Engineering Science. 62 (2007) 4277-4293.

[5] Birkhofer BH, Jeelani SAK, Windhab EJ, Ouriev B, Lisner K-J, Braun P, Zeng Y: Monitoring of fat crystallization process using UVP-PD technique, Flow Measurement and Instrumentation 19 (2008) 163-169.

[6] Xu H, Aidun CK: Characteristics of fiber suspension flow in a rectangular channel, International Journal of Multiphase Flow 31 (2005) 318-336.

[7] Jäsberg A: Flow behavior of fiber suspensions in straight pipes: new experimental techniques and multiphase modelling, PhD thesis, University of Jyväskylä, Finland, 2007.

[8] Wiklund J, Petterson AJ, Rasmuson A, Stading M: A comparative study of UVP and LDA techniques for pulp suspensions in pipe flow, A.I.Ch.E. Journal 52 (2006) 484-495.

[9] Wiklund J, Stading M: Application of in-line ultrasound Doppler-based UVP-PD Rheometry method to concentrated model and industrial suspensions, Flow Measurement and Instrumentation 19 (2008) 171-179.

[10] Pääkkö M, Ankerfors M, Kosonen H, Nykänen A, Ahola S, Österberg M, Ruokolainen J, Laine J, Larsson PT, Ikkala O, Lidström T: Enzymatic hydrolysis combined with mechanical shearing and high-pressure homogenization for nanoscale cellulose fibrils and strong gels, Biomacromolecules 6 (2007) 1934-1941.

[11] Tatsumi D, Ishioka S, Matsumoto, T: Effect of fiber concentration and axial ratio on the rheological properties of cellulose fiber suspensions, Journal of Society of Rheology 32 (2002) 27-32.

[12] White F, Fluid Mechanics, McGrawHill 2003.

[13] R. G. Cox and S. K. Hsu, The lateral migration of solid particles in a laminar flow near a plane, Intl. J. Multiphase Flow, 3:201--222, 1977

[14] P. Cherukat and J. B. McLaughlin, The inertial lift on a rigid sphere in a linear shear flow field near a flat wall, J. Fluid Mech., 263:1--18, 1994

[15] R.M. Soszynski and R.J. Kerekes, Elastic interlocking of nylon fibers suspended in liquid. Part 1. Nature of cohesion among fibers. Nord. Pulp Paper Res. J. 3 (1988), pp. 172–179.

[16] Martinez DM, Buckley K, Lindstrom A, Thiruvengadaswamy R, Olson JA, Ruth TJ, Kerekes RJ (2001) Characterizing the mobility of papermaking fibres during sedimentation. The Science of Papermaking 12th Fundamental Research Symposium. The Pulp and Paper Fundamental Research Society, Oxford, pp 25–254.

[17] Martinez DM, Kiiskinen H, Ahlman AK, Kerekes RJ (2003) On the mobility of flowing papermaking suspensions and its relationship to formation. J Pulp Pap Sci 29:341–347.

[18] A Metzner and J. Reed, “Flow of non-Newtonian fluids - correlation of the laminar, transition and turbulent-flow regions,” AIChE Journal, Vol. 1, No.4, 1955.

APPENDIX: METZNER REED REYNOLDS NUMBER

For ***Herschel-Bulkley fluids***, shear stress τ can be written as

$$\tau = \tau_0 + K\dot{\gamma}^n \quad . \tag{10}$$

where τ_0 is the yield stress, $\dot{\gamma}$ is the shear rate, *K* is the ***consistency index*** and *n* is the ***flow index***. Metzner and Reed defined the Reynolds number for the pipe flow of Hersley-Buckley fluids as [18]

$$\mathrm{Re}_{MR} = \frac{\rho u D}{\mu_w \left(\frac{3n+1}{4n}\right)\left(\frac{1}{1 - aX - bX^2 - cX^3}\right)} \tag{11}$$

where *u* is the average velocity and *D* is the pipe diameter and

$$\mu_w = \tau_w^{(n-1)/n}\left(\frac{K}{1-X}\right)^{1/n} \tag{12}$$

$$X = \frac{\tau_0}{\tau_w} \tag{13}$$

$$a = \frac{1}{2n+1} \tag{14}$$

$$b = \frac{2n}{(n+1)(2n+1)} \tag{15}$$

$$b = \frac{2n^2}{(n+1)(2n+1)} \tag{16}$$

$$\tau_w = \frac{D}{4}\nabla p \tag{17}$$

where ∇p is the pressure gradient in the tube. The flow is assumed to be turbulent, if

$$\mathrm{Re}_{MR} > 2200\,. \tag{18}$$

One should note that Eq. (18) is only an approximation of the complex transition behavior of Herschel-Bulkley fluids. It seems, however, to work well here. The slope of the loss curve of 0.3% MFC changes at *u*=1.3 m/s, indicating a transition to fully turbulent flow. And, indeed, Re_{MR} is about 2300 here. In Figure 8, the highest Reynolds numbers for 0.6%, 1.0% and 1.5% MFC flows are 300, 60, 1200, respectively. This explains why their loss curves haven't yet reached that of water, and that their velocity profiles are still quite blunt even at the highest flow rates.